International Journal for Housing Science and Its Applications
Publish August 6, 2025. Volume 46, Issue 3 Pages 8557-8569

https,//doi.org/10.70517/ijhsa463731

Spatio-temporal data mining reveals the dynamic regulatory mechanism of soil mineral ion-microbial interactions on phosphorus and sulfur cycles.

Lanxin Tang[1,*]
[1] School of Geographical Sciences, China West Normal University, Nanchong, Sichuan, 637002, China
Corresponding authors: (e-mail: lanxincwnu@163.com).

Abstract This study analyzes spatio-temporal data mining and prediction methods and further constructs a prediction model based on spatio-temporal analysis. The LSTM model is used to identify the temporal characteristics of the input data, and the time lag cross-correlation function is used to dynamically assess the correlation between time series. The spatial component is used to visualize the spatial lag relationship, and finally, the component models are integrated and coordinated through a fusion strategy. Based on the study of the effects of soil mineral ion-microbial interactions on phosphorus and sulfur cycles, this research achieves spatio-temporal distribution predictions for phosphorus and sulfur cycles. The abundance of functional genes related to organic phosphorus transformation in soil phosphorus cycle microorganisms, Shannon diversity indices, and soil mineral ions all showed significant positive correlations ($P < 0.05$). Similarly, as soil mineral ion concentrations increased, the abundance of sulfur reduction genes and sulfur oxidation genes in soil sulfur cycle microorganisms, as well as Shannon diversity indices, also increased. In grasslands, the density of phosphorus and sulfur ions exhibits a relatively stable annual distribution trend, while in paddy fields, the density of phosphorus and sulfur ions shows an increasing trend over time, being more susceptible to the influence of soil mineral ions. The prediction results of the phosphorus and sulfur cycles in non-saline-alkali grasslands for 2024 obtained from this model are generally consistent with the measured results.

Index Terms time lag cross-correlation function, LSTM model, spatio-temporal analysis model, phosphorus-sulfur cycle

I. Introduction

Soil microorganisms are an important component of ecosystems and play a significant role in the decomposition of soil organic matter and the fixation and conversion of nutrients, especially in the phosphorus and sulfur cycles and the regulation of phosphorus and sulfur element availability in agricultural ecosystems [1]-[4].

Phosphorus is one of the essential macronutrients for plant growth, serving as a key component of plant nucleotides, phospholipid bilayers, and proteins, and participating in various physiological and biochemical processes such as plant growth, cellular metabolism, photosynthetic phosphorylation, and the tricarboxylic acid cycle [5]-[7]. Microorganisms can promote the cycling of phosphorus in soil. Soil microorganisms possess multiple metabolic mechanisms that enable them to decompose organic phosphorus and convert it into inorganic phosphorus that is readily absorbed by plants [8], [9]. Additionally, microbial activity and the decomposition of organic matter produce acidic metabolic byproducts that lower soil pH. Changes in pH can influence the form and concentration of phosphorus in soil, promoting its activation and release, thereby increasing soil phosphorus availability [10]-[13]. Concurrently, soil microorganisms can secrete a series of hydrolases to promote the mineralization of soil organic phosphorus and release stable phosphorus, thereby driving the soil phosphorus cycle [14], [15].

Sulfur, as one of the macronutrients essential for plants, plays a crucial role in the synthesis of proteins, vitamins, and other substances vital to plant life [16]. Microorganisms also play a significant role in soil sulfur cycling, particularly the rhizosphere microbiome, which mediates sulfur exchange between soil and plants [17], [18]. In agricultural ecosystems, there is a close relationship between sulfate and hydrogen sulfide, and the sulfur cycling functions of microbial communities theoretically have the potential to enhance plant sulfur nutrient utilization, thereby improving crop yield and quality [19]-[21].

A wide variety of microorganisms are abundantly present in soil, playing crucial roles in maintaining soil health, enhancing soil fertility, improving soil environment, suppressing soil-borne diseases, promoting crop growth, and enhancing tolerance to abiotic stress [22]-[25]. Soil microorganisms drive the cycling of elements such as

phosphorus and sulfur in soil nutrient cycles, which are closely related to agricultural production and ecosystem functions. Tian, J., et al. introduced a microbial community capable of promoting soil phosphate solubilization (PSMs). By conducting a detailed analysis of the metabolic and enzymatic mechanisms underlying PSM mineralization of organic phosphorus and solubilization of inorganic phosphorus, they provided valuable insights into the chemical processes of soil phosphorus cycling [26]. Liu, L et al. demonstrated that long-term application of phosphorus fertilizers in soil reduces the expression of phosphorus cycle genes in functional microorganisms, proposing that altering soil microbial genes to drive soil nutrient cycling could ultimately achieve high-quality crop growth [27]. Hallama, M et al. investigated the phosphorus cycling mechanisms of soil microorganisms under cover crops, suggesting that applying these findings to agricultural management could tighten nutrient cycling in agricultural systems under different conditions, increase crop phosphorus nutrition and yield, while reducing fertilizer inputs [28]. Qi, J et al. studied the functional role and potential of microorganisms in phosphorus and sulfur cycling during the succession of soil biocrust (BSC) in desert ecosystems. Experimental results indicated that microbial communities and their functional genes were effectively expressed in BSC, enhancing microbial metabolic potential for phosphorus and sulfur elements [29]. Zhou, Z., et al. emphasized that microbial-mediated oxidation, reduction, and disproportionation reactions of sulfur compounds are crucial for biogeochemical cycles, while also assessing the complex involvement of microorganisms in sulfur dynamics [30]. Chaudhary, S et al. pointed out that microorganisms participate in sulfur cycling in soil through various processes such as oxidation, reduction, mineralization, fixation, and volatilization of sulfur compounds. Therefore, microorganisms can be utilized to enhance sulfur cycling between soil and plants, thereby effectively increasing crop yields [31].

As research continues to advance, scholars have recently discovered that soil mineral ions also participate in biogeochemical processes. Although microorganisms play a dominant role in phosphorus and sulfur cycling, the interaction between soil mineral ions and microorganisms is equally worthy of attention.

This study developed a predictive model based on spatio-temporal data modeling techniques to analyze the dynamic transformations in soil phosphorus and sulfur cycles. The model's core components include statistical, temporal, and spatial components. The LSTM model was used for temporal feature extraction and training of soil phosphorus and sulfur data, followed by evaluation of the correlation between time series using time-lagged cross-correlation functions to enhance the predictive performance of the temporal model. To accurately analyze the dynamic effects of soil mineral ion-microorganism interactions on phosphorus and sulfur cycling, the study measured soil properties, performed high-throughput sequencing on soil samples, and conducted spatio-temporal distribution predictions of soil phosphorus and sulfur cycling based on the research data.

II. Prediction model construction based on spatio-temporal data modeling technology

II. A. Knowledge related to spatio-temporal data mining

II. A. 1) Spatio-temporal data mining

Spatio-temporal data mining [32] refers to the process of exploring, analyzing, and extracting spatio-temporal relationships, patterns, and trends from data in the spatio-temporal domain. It combines data from both temporal and spatial dimensions, aiming to extract useful information and knowledge from spatio-temporal data to support decision-making, problem-solving, and prediction. The primary research objective of spatio-temporal data mining is to uncover hidden patterns, rules, and associations within spatio-temporal data through analysis, thereby gaining a deeper understanding of spatio-temporal processes. The main goal of spatio-temporal prediction is to forecast future spatio-temporal events, states, or trends based on past spatio-temporal data.

Given N region, T time steps, and C spatio-temporal tasks with historical state $x_{1:T}$, the goal of spatio-temporal prediction is to use model f_θ to mine the dependencies between time series and spatial locations in historical data to predict the spatio-temporal attributes $y_{T:H}$ for the next H time steps, i.e.:

$$x_{1:T} \xrightarrow{f_\theta} y_{T:H} \tag{1}$$

II. A. 2) Spatio-temporal prediction methods for data

Spatio-temporal prediction data mainly includes grid data and graph structure data, and these two types of data are usually determined by the collection equipment and application scenarios. Different deep learning methods tend to favor different types of data. For example, models based on convolutional neural network structures are good at handling matrix format data and usually perform well on grid data, while models based on graph rolls and networks can effectively extract the relationships between nodes by utilizing graph topological structures and usually perform better on graph structure data.

(1) Grid data

Raster data [33] is a data representation based on a regular grid or raster cells. It divides spatial areas into regular cells and assigns a value to each cell. In spatiotemporal forecasting, raster data can represent continuous or discrete phenomena, such as temperature, precipitation, and air quality index. Raster data typically uses a regular spatial resolution and is observed or measured at different time points.

(2) Graph-structured data

Graph-structured data is a data representation based on graphs, where nodes represent spatial locations or entities, and edges represent connections or relationships between them. In spatio-temporal forecasting, graph-structured data can represent complex spatio-temporal relationships, such as transportation networks, social networks, and logistics networks. Each node can have attributes that represent the node's characteristics or attribute information. Graph-structured data can be used to predict the evolution of node attributes, path planning, and the dynamic interactions between nodes.

II. B.Prediction model based on spatiotemporal analysis

Since the dynamics of the phosphorus-sulfur cycle are related to spatiotemporal factors, this paper proposes a spatiotemporal component fusion model for predicting the phosphorus-sulfur cycle, which describes temporal trends and spatial distributions based on statistical characteristics and integrates them into the prediction task. Specifically, the discussion is based on the following three components.

(1) Since observed values of phosphorus and sulfur cycles exhibit autocorrelation, this paper employs attribute representations from general statistical analysis to construct a statistical component model, analyzing the multidimensional statistical characteristics of phosphorus and sulfur cycles at independent time intervals.

(2) Considering the time lag and cross-correlation between soil mineral ions and microbial interactions, this paper constructs a temporal component model with three sub-components to describe the short-, medium-, and long-term periodic characteristics of time series.

(3) Based on spatial clustering analysis, the study evaluates the multivariate spatial dependence of interactions between soil mineral ions and microorganisms and constructs a spatial component model with correlation indicators as additional features. The model component architecture is shown in Figure 1.

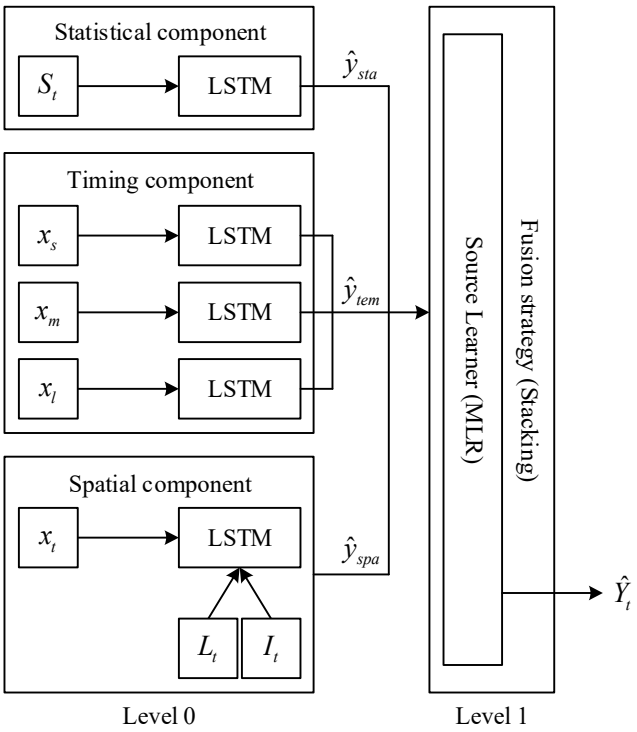

Figure 1: Model Component Architecture of our model

II. B. 1) Formalization of the problem

Learn about static property characteristics and dynamic spatio-temporal characteristics from a holistic perspective, and abstract the spatio-temporal dependencies between soil mineral ions, microorganisms, and phosphorus-sulfur cycles.

Formulating the aggregation patterns of soil mineral ions and microorganisms into a spatiotemporal structure, each time slice t corresponds to a spatial map $G=(V,A)$, which includes a grid node set V of soil mineral ions and microorganisms, as well as an adjacency matrix $A \in \mathbb{R}^{N\times N}$ with N grid nodes. Assuming the length of the time series is T, the temporal records of phosphorus and sulfur cycles are represented as $x_t \in \mathbb{R}^{D\times N}(t=1,2,...,T)$, where each record x_t contains D-dimensional features distributed across N nodes. x_i^{di} denotes the observed value of feature d at node i in the t th time step. This risk prediction problem can be formalized as follows: given the corresponding features $X=(x_1,x_2,...,x_\tau)$ over τ time steps, predict the number $\hat{y}_{\tau+\gamma}$ of interactions between soil mineral ions and microorganisms and the phosphorus-sulfur cycle, where γ represents the prediction window length.

II. B. 2) Statistical Component Construction

Given that the dynamics of the phosphorus-sulfur cycle exhibit autocorrelation, this paper proposes a statistical component model to describe the statistical characteristics of phosphorus-sulfur cycle sequences. The dynamics of the phosphorus-sulfur cycle are influenced by the interaction between soil mineral ions and microorganisms. Therefore, the time window is set to the cycle period length, and the statistical characteristics within the window are calculated. In addition, since the dynamics of the phosphorus-sulfur cycle exhibit seasonality, the input variables of the statistical component model are constructed as follows:

$$S_t=\left[Sum_t,Incr_t,Mean_t,Med_t,Max_t,Min_t,SPLY_t\right] \tag{2}$$

The subscript indicates the time step.

As the output of the forget gate, f_t determines the forget probability of the hidden unit state in the previous layer through a nonlinear activation function σ, with a value range of [0, 1]. $W \in \mathbb{R}^{H\times H}$ and $U \in \mathbb{R}^{H\times D}$ represent the coefficient matrix of the hidden state and input vector, where H is the number of hidden units and b is the bias parameter. i_t and f_t act on the previous state C_{t-1} and the candidate vector $\tilde{C}_t$ obtained at the current time through the tanh activation function, respectively, as weight parameters to update the cell state C_t, where $\odot$ is the Hadamard product. h_t is updated through the output gate o_i to determine the part of the cell state C_i activated by tanh. The output layer calculates the output value $\hat{y}_t$ through the weighted connection of the hidden layer sequence $h_1,h_2,...,h_t$.

II. B. 3) Sequential Component Construction

This paper proposes a solution that combines short-, medium-, and long-term cycle characteristics, dividing the time series into three stages for modeling to flexibly capture the impact of temporal dependencies on forecasting tasks. Specifically, a time series component model comprising three subcomponents is constructed to describe the associated characteristics of short-, medium-, and long-term cycles, with the corresponding time periods represented as T_s,T_m,T_l.

This paper selects the Spearman rank correlation coefficient as a measure of monotonic correlation to quantify the inter-sequence correlation at a $k-th$ -step lag. Assuming that time series $X_1,X_2,...,X_T$ and $Y_1,Y_2,...,Y_T$ represent the mosquito-borne mineral ion index sequence and the phosphorus-sulfur cycle sequence, respectively, the temporal lag correlation between X_t and Y_{t+k} is defined as:

$$\rho_{XY}(k)=\begin{cases}1-\dfrac{6\sum_{t=1}^{T-k}(\tilde{Y}_{t+k}-\tilde{X}_t)^2}{(T-k)((T-k)^2-1)}, & k\geq 0\\ 1-\dfrac{6\sum_{t=1-k}^{T}(\tilde{Y}_{t+k}-\tilde{X}_t)^2}{(T+k)((T+k)^2-1)}, & k<0\end{cases} \tag{3}$$

where $\tilde{Y}_{t+k}$ and $\tilde{X}_i$ represent the positions of Y_{t+k} and X_t after sorting, respectively, and T represents the length of the time series. Values range from -1 to 1, with the absolute value indicating the degree of correlation.

II. B. 4) Spatial Component Construction

Divide the geographic space into N grids and extract spatial factors based on the spatial distribution of cases in the actual scenario. By analyzing the correlation between the phosphorus-sulfur cycle index y in Region i and the mineral ion index x in the adjacent Region j, spatial lag is extended to a two-dimensional dimension, i.e., $L_t(y_i) = \sum_j^N a_{ij} x_j$, where y_i and x_j are both standardized. A self-connection approach is adopted to consider the influence of the node itself and calculate the internal correlation. The specific method involves obtaining an adjacency matrix A as spatial weight values based on the geographical distribution of regions, where a_{ij} = 1 indicates that regions i and j are adjacent, and A is updated by adding self-connections $A + I_N$:

$$A = A + I_N = \begin{pmatrix} a_{11} & a_{12} & \cdots & a_{1n} \\ a_{21} & a_{22} & \cdots & a_{2n} \\ \vdots & \vdots & \ddots & \vdots \\ a_{n1} & a_{n2} & \cdots & a_{nn} \end{pmatrix} + \begin{pmatrix} 1 & 0 & \cdots & 0 \\ 0 & 1 & \cdots & 0 \\ \vdots & \vdots & \ddots & \vdots \\ 0 & 0 & \cdots & 1 \end{pmatrix} \tag{4}$$

The spatial cross-correlation coefficient between phosphorus-sulfur cycle numbers and microorganisms was calculated using the binary local Moran index:

$$I_i = C\tilde{y}_i \sum_j^N a_{ij} \tilde{x}_j \tag{5}$$

Among them, $\tilde{x}_i = x_i - \overline{x}$, $\tilde{y}_j = y_j - \overline{y}$, and C are used for standardization. $I_i > 0$ indicates that there is a spatial positive correlation between the number of cases in region i and microorganisms in adjacent regions, and $\sum_j^N a_v \tilde{x}_j$ indicates the corresponding spatial lag value.

ConvLSTM was selected as the spatial component model to learn the spatial relationships between the phosphorus-sulfur cycle and microorganisms. ConvLSTM is based on the LSTM structure but uses convolution instead of state full connection mode. Compared with LSTM, it can further extract spatial information. The update formula is:

$$\begin{cases} f_t = \sigma(W_{hf} * h_{t-1} + W_{xf} * x_t + W_{cf} \circ C_{t-1} + b_f) \\ i_t = \sigma(W_{hi} * h_{t-1} + W_{xi} * x_t + W_{ci} \circ C_{t-1} + b_i) \\ C_t = f_t \circ C_{t-1} + i_t \circ \tanh(W_{hc} * h_{t-1} + W_{xc} * x_t + b_c) \\ o_t = \sigma(W_{ho} * H_{t-1} + W_{xo} * x_t + W_{co} \circ C_t + b_o) \\ h_t = o_t \tanh(C_t) \end{cases} \tag{6}$$

The asterisk (*) denotes a convolution operation, and $\circ$ denotes a Hadamard product. This can be interpreted as meaning that the amount of phosphorus and sulfur cycling in a given region is not only related to the current region, but also influenced by other regions.

II. B. 5) Component Fusion Strategy

In order to integrate the advantages of each component learner to improve performance, each individual learner should have uniqueness and accuracy. This paper constructs statistical, temporal, and spatial components to capture features in three dimensions: statistical attributes, temporal trends, and spatial distribution. Assuming that the output sequence $\hat{y} = [\hat{y}_1, \hat{y}_2, ..., \hat{y}_T]^T$, T represents the length of the time series. For output $\hat{y}_t \in \square$, the multiple linear regression model can be expressed as:

$$\hat{y}_t = \omega_0 + \omega_1 \hat{y}_t^1 + \omega_2 \hat{y}_t^2 + ... + \omega_n \hat{y}_t^n \tag{7}$$

Among them, there is a total of n prediction model, $\hat{y}_i^{'}$ indicates the prediction result of the i rd model at time t, and ω_i is used to measure the impact of different component models on the prediction results.

III. Research on the dynamic effects of soil mineral ions and microorganisms on phosphorus and sulfur cycles

III. A. Study Area and Experimental Design

The study area for this experiment is located at the XX Wetland Ecosystem Field Research and Observation Station (110°40′E, 35°56′N), which has a temperate monsoon climate with an average annual precipitation of 653.44 mm. Sampling was conducted between 2014 and 2024. Six sampling areas, each containing “grassland, dry field, paddy field, wetland, forest land, and bare land,” were selected and named BJ1-3, NW1-2, LF1-2, CJ1-3, LS1-3, and TDZ1-3, respectively, totaling 16 samples. The soil in the study area is slightly acidic, with mineral ion concentrations ranging from approximately 50 to 300 mg/kg.

III. B. Soil sample collection and pretreatment

Using a 5 cm diameter drill bit, surface soil samples (0–10 cm) were collected from 2014 to 2024, i.e., two years after the construction of the OTCs. During sampling, plant roots and rocks were removed from the soil and placed in sealed bags for subsequent soil property analysis. Simultaneously, 1–3 g of soil samples were collected using a sterile sampling spoon and placed in 2 mL sterile PVC tubes for subsequent microbial analysis. All soil samples were placed in ice boxes and transported to the laboratory within 2 hours. Soil samples for microbial analysis were stored at -80°C; approximately one-quarter of the samples for soil property analysis were stored at -20°C for measuring soil water content (SWC), salinity, and inorganic nitrogen content; the remaining samples were air-dried, with a portion sieved through a 2 mm sieve for future use.

III. C. Soil Sample Measurement and Analysis

III. C. 1) Determination of physical and chemical properties

Mix soil with deionized water in a 1:5 ratio, stir with a magnetic stirrer for 1 minute, then let it sit for 40 minutes. Immerse the calibrated pH meter electrode ball in the supernatant and measure the pH value of the soil. Fresh soil was dried using the oven drying method at 105°C. The fresh and dried soil weights, along with the aluminum container mass, were recorded and calculated using a formula to determine the soil's moisture content. The TOC-L analyzer was used to measure the soil's TOC and TN content. Mix 5 g of fresh soil with 25 mL of 2 mol/L potassium chloride solution, shake for 1 hour, then centrifuge for 30 minutes. Extract the supernatant and measure the soil NH_4^+–N and NO_3^-N content using a flow analyzer. Digest with H_2SO_4–$HClO_4$ solution and determine the TP content using a spectrophotometer.

III. C. 2) High-throughput sequencing

Use a DNA kit to extract DNA from soil samples. Use the forward primer 519F (5′-CAGCCGCCGCGGTAA-3′), ITS3F (5′-GCATCGATGAAGAACGCAGC-3′), and reverse primer 915R (5′-GTGCTCCCCCGCCAATTCCT-3′) and ITS4R (5′-TCCTCCGCTTATTGATATGC-3′) to amplify the V4–V5 region of archaea and the ITS2 region of fungi using a BioRad S1000 PCR instrument. PCR products were detected by 1% agarose gel electrophoresis, and concentrations were compared using GeneTools before mixing. PCR mixture products and target DNA fragments were recovered using a recovery kit and buffer. Amplified fragment libraries were constructed according to the standard procedure of the NEBNext® Ultra™ DNA Library Prep Kit for Illumina®, and the libraries were sequenced using the Illumina Hiseq platform with PE250 read lengths. Quality filtering was performed using Trimmomatic software (V0.33), assembly was performed using FLASH software (V1.2.11), and effective assembled fragments were obtained using Mothur software (V1.35.1). Using the usearch software (V10) and clustering at 97% similarity, multiple operational taxonomic units (OTUs) were identified. The assign_taxonomy.py script from Qiime was used to remove chimeras, and the representative sequences of the OTUs were compared with the Silva and Unite databases. The RDP Classifier and Blast comparison methods were used to obtain species annotation information for 16S and ITS, respectively.

III. C. 3) Determination of soil microbial functional genes and data processing

This study utilized the GeoChip platform from Agilent to measure soil microbial functional genes. Soil sample genomic DNA extraction, quality assessment, and final concentration quantification were performed using a kit (Guangdong Magigene Biotechnology Co., Ltd., Guangzhou, China), Nanodrop One (Thermo Fisher Scientific, Waltham, USA), and FLUOstar Optima microplate reader (BMG Labtech, Jena, Germany), respectively. DNA was labeled with Cy3 and purified using random primers, the Klenow fragment of DNA polymerase I, and the QIA kit (Qiagen, Valencia, CA, USA). The DNA was dried at 52°C for 50 minutes in the Labconco Centrivap Concentrator (Labconco Corp., Kansas City, MO), diluted, incubated at 90°C for 10 minutes, and maintained at 45°C until hybridization. The hybridization station (MAUI, BioMicro Systems, Salt Lake City, UT, USA) was preheated at 45°C for 10 minutes, and the labeled DNA samples were placed on the array for hybridization for approximately 20 hours. The chip was scanned using the NimbleGen MS200 instrument to obtain optical signals. The optical signals were

converted into digital signals using ImaGene software, followed by inter-array normalization and false positive removal. Signal points with a signal-to-noise ratio (SNR) < 2 were removed to obtain the raw probe signal intensity. The raw probe signal intensity was standardized to obtain the standardized probe signal intensity. The standardized probe signal intensity for each gene was then aggregated to obtain the gene signal intensity.

III. D. Dynamic effects of soil mineral ions and microorganisms on phosphorus and sulfur cycling

III. D. 1) Spatial characteristics of microbial functional genes in soil phosphorus cycling

(1) Abundance of microbial functional genes involved in soil phosphorus cycling and Shannon diversity

Soil phosphorus cycling functions include organic phosphorus conversion, organic phosphorus synthesis, and inorganic phosphorus degradation. The abundance of microbial functional genes involved in soil phosphorus cycling is shown in Table 1. The table shows that the abundance of soil microbial genes is highest for inorganic phosphorus degradation genes, followed by inorganic phosphorus synthesis genes, and then organic phosphorus conversion genes.

Table 1: Soil phosphorus circulation microbe function gene abundance

Sampling area	Sample number	Organic phosphorus conversion	Inorganic phosphorus synthesis	Inorganic phosphorus degradation
BJ	BJ 1	147.03	325.41	914.18
	BJ 2	138.12	298.32	881.91
	BJ 3	143.05	294.79	835.15
NW	NW 1	140.55	315.49	861.84
	NW 2	131.55	320.69	851.01
LF	LF 1	119.59	282.11	766.61
	LF 2	139.47	309.9	889.86
CJ	CJ 1	129.73	305.01	800.85
	CJ 2	125.39	301.05	765.79
	CJ 3	111.42	259.21	732.83
LS	LS 1	129.68	296.92	782.6
	LS 2	136.29	285.28	820.78
	LS 3	127.79	294.18	788.49
TDZ	TDZ 1	86.93	207.59	564.24
	TDZ 2	95.01	215.24	573.1
	TDZ 3	106.66	232.13	637.84

Table 2: Soil phosphorus cycle microorganism function gene shannon diversity index

Sampling area	Sample number	Organic phosphorus conversion	Inorganic phosphorus synthesis	Inorganic phosphorus degradation
BJ	BJ 1	4.8041	5.6015	6.6997
	BJ 2	4.7936	5.5975	6.6985
	BJ 3	4.8024	5.6008	6.7017
NW	NW 1	4.7962	5.6051	6.7064
	NW 2	4.7979	5.6004	6.6998
LF	LF 1	4.7963	5.6022	6.7009
	LF 2	4.8008	5.5999	6.7016
CJ	CJ 1	4.8036	5.6042	6.7015
	CJ 2	4.7976	5.5937	6.7036
	CJ 3	4.8004	5.6003	6.7004
LS	LS 1	4.7967	5.5929	6.6975
	LS 2	4.7969	5.6017	6.7021
	LS 3	4.8026	5.6016	6.6992
TDZ	TDZ 1	4.8029	5.6011	6.7035
	TDZ 2	4.7991	5.5983	6.7054
	TDZ 3	4.8031	5.5911	6.6983

The Shannon diversity index of soil phosphorus cycle microbial functional genes is shown in Table 2. The Shannon diversity index of soil phosphorus cycle microbial functional genes and gene abundance showed the same pattern, but there were no significant differences between the different plots.

(2) Relationship between soil phosphorus cycle microbial functional genes and soil mineral ions

① Relationship between soil phosphorus cycle microbial functional gene abundance and soil mineral ions

The relationship between soil phosphorus cycle microbial functional gene abundance and soil mineral ions is shown in Figure 2. The results indicate that the abundance of soil phosphorus cycle microbial organic phosphorus conversion, inorganic phosphorus synthesis, and inorganic phosphorus degradation genes is significantly positively correlated with soil mineral ions ($P < 0.05$).

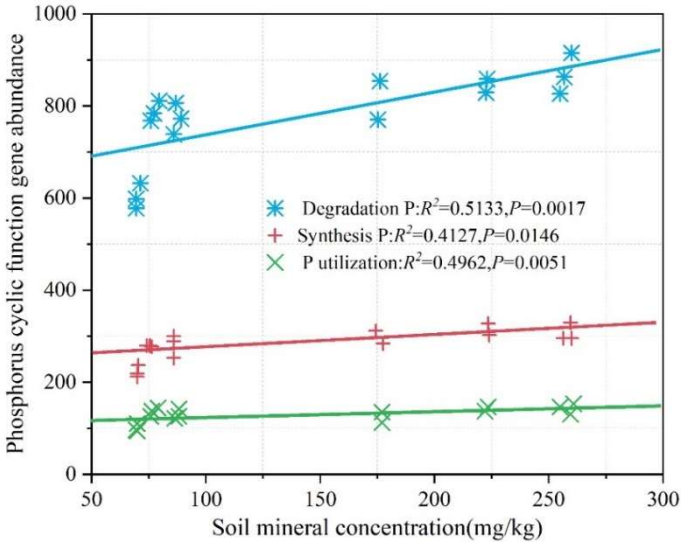

Figure 2: The relationship between phosphorus circulation and soil mineral ion

②Relationship between the Shannon diversity index of soil phosphorus cycle microbial functional genes and soil mineral ions

The relationship between the Shannon diversity index of soil phosphorus cycle microbial functional genes and soil mineral ions is shown in Figure 3. The results indicate that the Shannon diversity index of soil phosphorus cycle microbial organic phosphorus conversion, inorganic phosphorus synthesis, and inorganic phosphorus degradation genes is significantly positively correlated with soil mineral ions ($P < 0.05$).

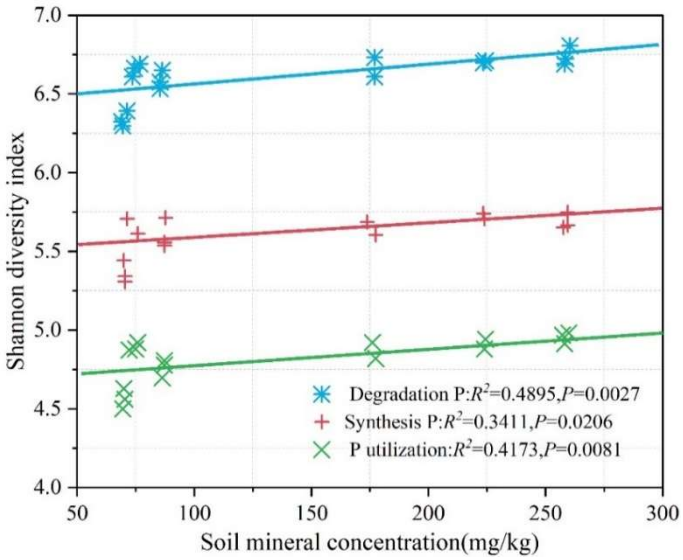

Figure 3: The relationship between the diversity index and the soil mineral ion

III. D. 2) Spatial characteristics of microbial functional genes in soil sulfur cycling

Soil sulfur cycle microbial functions include sulfur reduction and sulfur oxidation.

(1) Soil sulfur cycle microbial functional gene abundance and Shannon diversity

Soil sulfur cycle microbial functional gene abundance and Shannon diversity indices are shown in Table 3. As can be seen from the table, soil sulfur cycle microbial functional gene abundance and Shannon diversity indices both show that sulfur reduction genes are higher than sulfur oxidation genes.

Table 3: Gene abundance and shannon diversity index

Sampling area	Sample number	Gene abundance		Genetic diversity	
		Sulfur reduction	Sulfur oxidation	Sulfur reduction	Sulfur oxidation
BJ	BJ 1	1506.14	638.69	7.2047	6.3958
	BJ 2	1327.42	612.05	7.1967	6.4008
	BJ 3	1324.66	564	7.2016	6.402
NW	NW 1	1566.26	648.98	7.1952	6.3966
	NW 2	1551.12	647.64	7.1826	6.3959
LF	LF 1	1411.58	615.27	7.2059	6.3993
	LF 2	1510.96	642.93	7.2014	6.4033
CJ	CJ 1	1430.64	621.46	7.1943	6.3927
	CJ 2	1418.8	590.23	7.1921	6.3987
	CJ 3	1355.46	587.21	7.1982	6.3974
LS	LS 1	1392.66	595.99	7.1774	6.3955
	LS 2	1216.09	556.58	7.2073	6.3964
	LS 3	1435.06	614.05	7.1908	6.3981
TDZ	TDZ 1	943.99	448.4	7.2011	6.3968
	TDZ 2	989.66	431.95	7.1975	6.4033
	TDZ 3	1035.44	479.61	7.2031	6.3933

(2) Relationship between soil sulfur cycle microbial functional genes and soil mineral ions

① Relationship between soil sulfur cycle microbial functional gene abundance and soil mineral ions

The relationship between soil sulfur cycle microbial functional gene abundance and soil mineral ions is shown in Figure 4. The results indicate that the correlation coefficients between sulfur-reducing gene abundance and sulfur-oxidizing gene abundance and soil mineral ions are 0.2954 and 0.3119, respectively, with P-values of 0.0217 and 0.0154 < 0.05. Clearly, sulfur-reducing gene abundance and sulfur-oxidizing gene abundance are significantly positively correlated with soil mineral ions ($P < 0.05$).

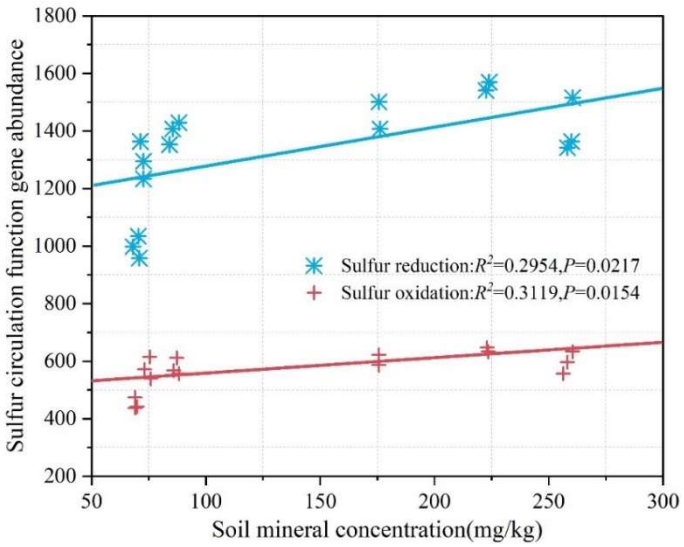

Figure 4: The relationship between the gene abundance and the soil mineral ion

②Relationship between the Shannon diversity index of soil sulfur cycle microbial functional genes and soil mineral ions

The relationship between the Shannon diversity index of soil sulfur cycle microbial functional genes and soil mineral ions is shown in Figure 5. The results indicate that the correlation coefficients between the Shannon diversity indices of soil sulfur-reducing genes and sulfur-oxidizing genes and soil mineral ions are 0.2833 and 0.3024, respectively, with significance P-values of 0.0209 and 0.0211 < 0.05, indicating that the Shannon diversity indices of sulfur-reducing genes and sulfur-oxidizing genes are significantly positively correlated with soil mineral ions (P < 0.05).

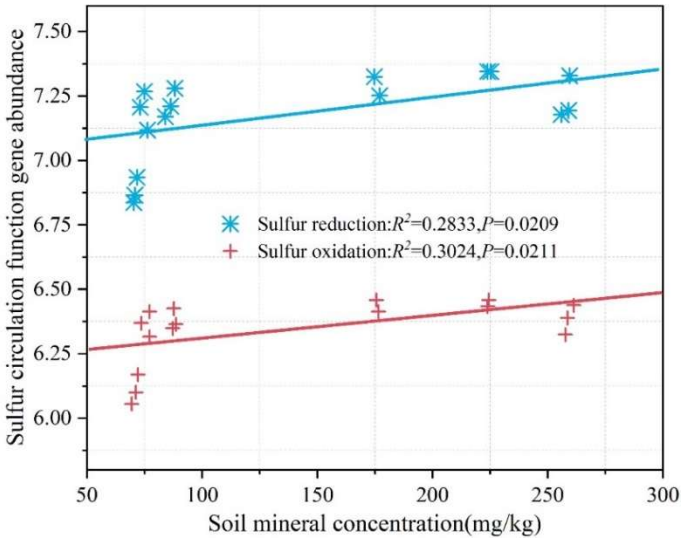

Figure 5: The relationship between the diversity index and the soil mineral ion

The results of the study indicate that, in terms of soil microbial functional gene abundance and Shannon diversity index, sulfur cycle functional genes > phosphorus cycle functional genes, and the corresponding secondary functional genes also generally follow this pattern. This suggests that phosphorus and sulfur cycles play a significant role in material cycling and energy transfer within ecosystems. Regarding the spatial distribution of soil microbial functional gene abundance and Shannon diversity index, except for a few functional genes that showed no significant positive correlation with soil mineral ions, most functional genes exhibited a significant positive correlation with soil mineral ions. This highlights the unique distribution pattern of soil mineral ions and microbial functional genes in ecosystems, which directly or indirectly influences the processes of soil phosphorus and sulfur cycling.

IV. Analysis of the results of spatio-temporal distribution predictions for soil phosphorus and sulfur cycles

To conduct a more detailed analysis of the dynamic effects of soil mineral ion and microbial interactions on phosphorus and sulfur cycling, this section categorizes the different land use types mentioned earlier (this section only selects grassland and paddy fields for predictive assessment) into three types—“non-saline-alkali land, slightly saline-alkali land, and moderately saline-alkali land”—based on their soil mineral ion concentrations, and conducts a survey and field measurement analysis of the spatiotemporal distribution of soil phosphorus and sulfur from 2014 to 2024.

The annual changes in the density of phosphorus and sulfur ions in soil from 2014 to 2024 are shown in Figure 6, where (a) and (b) represent grassland and paddy fields, respectively. The measured results indicate that for grassland, the distribution of phosphorus and sulfur ion density is relatively stable. The dynamic cycle of phosphorus and sulfur in grassland soil is significantly influenced by soil mineral ions. The phosphorus and sulfur ion density and microbial abundance in non-saline-alkali grassland soil are significantly higher than those in saline-alkali grassland soil. The phosphorus and sulfur ion densities in mildly saline-alkali grassland and moderately saline-alkali grassland are similar.

For paddy fields, the phosphorus and sulfur ion densities show an increasing trend year by year. In years when land use remains unchanged, changes in soil mineral ions are minimal, and microbial activity decreases significantly. After microbial functional genes are significantly enhanced, interactions between soil mineral ions and microorganisms become more frequent, leading to a significant enhancement of the phosphorus and sulfur cycle.

However, as the years progress, the cycle of soil phosphorus and sulfur cycling becomes significantly longer. This result may be related to the excessive application of chemical fertilizers such as phosphorus fertilizers and urea. For example, the excessive use of urea and phosphorus fertilizers can lead to increased levels of phosphorus and sulfur elements in the soil, exacerbating soil salinization and compaction, thereby reducing the activity of soil functional microorganisms such as phosphorus and sulfur, and ultimately prolonging the cycle of phosphorus and sulfur cycling.

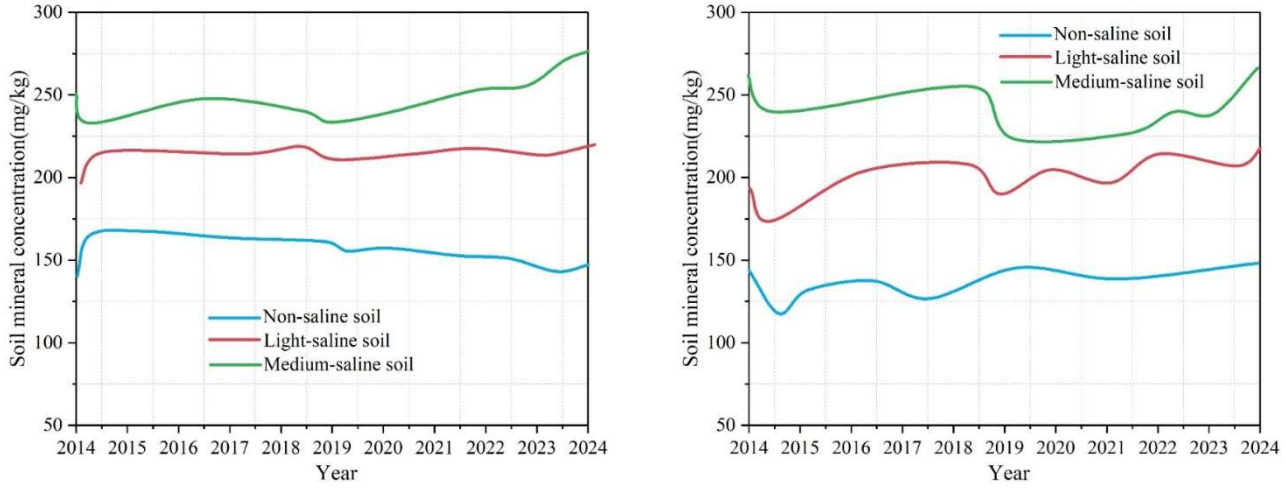

(a) Grass (b) Water field

Figure 6: The density of phosphorus sulfur ions in soil varies year by year

This section compares data from non-saline-alkali grasslands (abbreviated as N-G) in 2024. The results of the dynamic effects of soil mineral ions and microorganisms on phosphorus and sulfur cycling are shown in Figure 7, where (a) and (b) represent actual values and predicted values, respectively. Red represents the activity range of microorganisms, green represents phosphorus and sulfur cycling, and blue represents the distribution of soil mineral ions. From the measured results of the phosphorus and sulfur cycles in N-G grasslands in 2024, it can be observed that both microbial activity and soil mineral ion distribution areas are generally associated with phosphorus and sulfur cycling processes. The predicted results from this model also show similar patterns, with the predicted values closely aligning with the actual values. Both indicate that the distribution of microorganisms and soil mineral ions influences phosphorus and sulfur cycling, and in areas where these two factors interact, the cycling of phosphorus and sulfur in the soil becomes more closely intertwined.

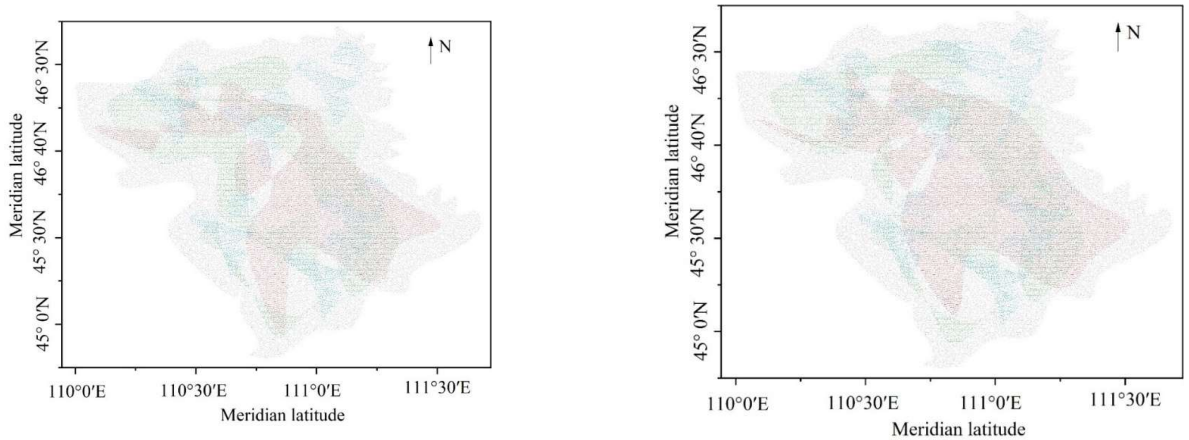

(a) True value (b) Predictive value

Figure 7: Effects of soil mineral ions and microorganisms on phosphoric sulfur cycle

V. Conclusion

The article introduces knowledge related to spatio-temporal data mining and utilizes spatio-temporal data modeling techniques to construct a spatio-temporal analysis and prediction model. The statistical component model describes the statistical characteristics of the spatio-temporal sequence of the phosphorus-sulfur cycle, while the temporal component model captures the impact of temporal dependencies on phosphorus-sulfur cycle prediction tasks in a phased manner. Combined with the spatial component model, this enables the visualization of spatial lag relationships in phosphorus-sulfur cycle data. Based on the research findings regarding the dynamic effects of soil mineral ions and microorganisms on the phosphorus-sulfur cycle, a spatio-temporal distribution analysis of the soil phosphorus-sulfur cycle is conducted.

The abundance of genes involved in organic phosphorus conversion, inorganic phosphorus synthesis, and inorganic phosphorus degradation in phosphorus-cycling microorganisms showed a significant positive correlation with soil mineral ion concentrations, with correlation coefficients ranging from 0.0017 to 0.0146. For sulfur cycle microorganisms, the abundance of sulfur reduction genes and sulfur oxidation genes increases with rising soil mineral ion concentrations, with correlation coefficients of 0.2833 and 0.3024, respectively, and both passed significance tests. Under different regional conditions, the annual distribution trends of phosphorus and sulfur ion densities vary, but all are influenced by mineral ions. The spatio-temporal analysis prediction model shows good predictive performance, with the predicted values for phosphorus and sulfur cycling in non-saline-alkali grasslands at different latitudes and longitudes in 2024 aligning well with the actual values.

References

[1] Tang, S., Ma, Q., Marsden, K. A., Chadwick, D. R., Luo, Y., Kuzyakov, Y., ... & Jones, D. L. (2023). Microbial community succession in soil is mainly driven by carbon and nitrogen contents rather than phosphorus and sulphur contents. Soil Biology and Biochemistry, 180, 109019.

[2] Basu, S., Kumar, G., Chhabra, S., & Prasad, R. (2021). Role of soil microbes in biogeochemical cycle for enhancing soil fertility. In New and future developments in microbial biotechnology and bioengineering (pp. 149-157). Elsevier.

[3] Luo, G., Xue, C., Jiang, Q., Xiao, Y., Zhang, F., Guo, S., ... & Ling, N. (2020). Soil carbon, nitrogen, and phosphorus cycling microbial populations and their resistance to global change depend on soil C: N: P stoichiometry. Msystems, 5(3), 10-1128.

[4] Gerson, J. R., & Hinckley, E. L. S. (2023). It is time to develop sustainable management of agricultural sulfur. Earth's Future, 11(11), e2023EF003723.

[5] Sun, Y., Jiang, Y., Li, Y., Wang, Q., Zhu, G., Yi, T., ... & Zhang, P. (2024). Unlocking the potential of nanoscale sulfur in sustainable agriculture. Chemical science, 15(13), 4709-4722.

[6] Jing, Z., Chen, R., Wei, S., Feng, Y., Zhang, J., & Lin, X. (2017). Response and feedback of C mineralization to P availability driven by soil microorganisms. Soil Biology and Biochemistry, 105, 111-120.

[7] Wei, X., Hu, Y., Razavi, B. S., Zhou, J., Shen, J., Nannipieri, P., ... & Ge, T. (2019). Rare taxa of alkaline phosphomonoesterase-harboring microorganisms mediate soil phosphorus mineralization. Soil Biology and Biochemistry, 131, 62-70.

[8] Hemkemeyer, M., Schwalb, S. A., Heinze, S., Joergensen, R. G., & Wichern, F. (2021). Functions of elements in soil microorganisms. Microbiological Research, 252, 126832.

[9] Baumann, K., Jung, P., Samolov, E., Lehnert, L. W., Büdel, B., Karsten, U., ... & Leinweber, P. (2018). Biological soil crusts along a climatic gradient in Chile: Richness and imprints of phototrophic microorganisms in phosphorus biogeochemical cycling. Soil Biology and Biochemistry, 127, 286-300.

[10] Ding, W., Cong, W. F., & Lambers, H. (2021). Plant phosphorus-acquisition and-use strategies affect soil carbon cycling. Trends in Ecology & Evolution, 36(10), 899-906.

[11] Gao, D., Bai, E., Yang, Y., Zong, S., & Hagedorn, F. (2021). A global meta-analysis on freeze-thaw effects on soil carbon and phosphorus cycling. Soil Biology and Biochemistry, 159, 108283.

[12] Lang, F., Krüger, J., Amelung, W., Willbold, S., Frossard, E., Bünemann, E. K., ... & Chmara, I. (2017). Soil phosphorus supply controls P nutrition strategies of beech forest ecosystems in Central Europe. Biogeochemistry, 136, 5-29.

[13] Liang, J. L., Liu, J., Jia, P., Yang, T. T., Zeng, Q. W., Zhang, S. C., ... & Li, J. T. (2020). Novel phosphate-solubilizing bacteria enhance soil phosphorus cycling following ecological restoration of land degraded by mining. The ISME journal, 14(6), 1600-1613.

[14] Wu, X., Rensing, C., Han, D., Xiao, K. Q., Dai, Y., Tang, Z., ... & Zhang, F. (2022). Genome-resolved metagenomics reveals distinct phosphorus acquisition strategies between soil microbiomes. Msystems, 7(1), e01107-21.

[15] Dai, Z., Liu, G., Chen, H., Chen, C., Wang, J., Ai, S., ... & Xu, J. (2020). Long-term nutrient inputs shift soil microbial functional profiles of phosphorus cycling in diverse agroecosystems. The ISME journal, 14(3), 757-770.

[16] Sharma, R. K., Cox, M. S., Oglesby, C., & Dhillon, J. S. (2024). Revisiting the role of sulfur in crop production: A narrative review. Journal of Agriculture and Food Research, 15, 101013.

[17] Wu, B., Liu, F., Fang, W., Yang, T., Chen, G. H., He, Z., & Wang, S. (2021). Microbial sulfur metabolism and environmental implications. Science of The Total Environment, 778, 146085.

[18] Wang, M., Wang, L., Shi, H., Liu, Y., & Chen, S. (2021). Soil bacteria, genes, and metabolites stimulated during sulfur cycling and cadmium mobilization under sodium sulfate stress. Environmental Research, 201, 111599.

[19] Ma, Q., Wen, Y., Pan, W., Macdonald, A., Hill, P. W., Chadwick, D. R., ... & Jones, D. L. (2020). Soil carbon, nitrogen, and sulphur status affects the metabolism of organic S but not its uptake by microorganisms. Soil Biology and Biochemistry, 149, 107943.

[20] Dahl, C. (2020). A biochemical view on the biological sulfur cycle. Environmental technologies to treat sulfur pollution: principles and engineering, 2, 55-96.

[21] Zecchin, S., Corsini, A., Martin, M., & Cavalca, L. (2017). Influence of water management on the active root-associated microbiota involved in arsenic, iron, and sulfur cycles in rice paddies. Applied Microbiology and Biotechnology, 101, 6725-6738.

[22] Sahu, N., Vasu, D., Sahu, A., Lal, N., & Singh, S. K. (2017). Strength of microbes in nutrient cycling: a key to soil health. Agriculturally important microbes for sustainable agriculture: Volume I: Plant-soil-microbe nexus, 69-86.
[23] Yadav, A. N., Kour, D., Kaur, T., Devi, R., Yadav, A., Dikilitas, M., ... & Saxena, A. K. (2021). Biodiversity, and biotechnological contribution of beneficial soil microbiomes for nutrient cycling, plant growth improvement and nutrient uptake. Biocatalysis and Agricultural Biotechnology, 33, 102009.
[24] Philippot, L., Chenu, C., Kappler, A., Rillig, M. C., & Fierer, N. (2024). The interplay between microbial communities and soil properties. Nature Reviews Microbiology, 22(4), 226-239.
[25] Neemisha, & Sharma, S. (2022). Soil enzymes and their role in nutrient cycling. In Structure and functions of Pedosphere (pp. 173-188). Singapore: Springer Nature Singapore.
[26] Tian, J., Ge, F., Zhang, D., Deng, S., & Liu, X. (2021). Roles of phosphate solubilizing microorganisms from managing soil phosphorus deficiency to mediating biogeochemical P cycle. Biology, 10(2), 158.
[27] Liu, L., Gao, Y., Yang, W., Liu, J., & Wang, Z. (2024). Community metagenomics reveals the processes of nutrient cycling regulated by microbial functions in soils with P fertilizer input. Plant and Soil, 499(1), 139-154.
[28] Hallama, M., Pekrun, C., Lambers, H., & Kandeler, E. (2019). Hidden miners–the roles of cover crops and soil microorganisms in phosphorus cycling through agroecosystems. Plant and soil, 434, 7-45.
[29] Qi, J., Liu, Y., Wang, Z., Zhao, L., Zhang, W., Wang, Y., & Li, X. (2021). Variations in microbial functional potential associated with phosphorus and sulfur cycling in biological soil crusts of different ages at the Tengger Desert, China. Applied Soil Ecology, 165, 104022.
[30] Zhou, Z., Tran, P. Q., Cowley, E. S., Trembath-Reichert, E., & Anantharaman, K. (2025). Diversity and ecology of microbial sulfur metabolism. Nature Reviews Microbiology, 23(2), 122-140.
[31] Chaudhary, S., Sindhu, S. S., Dhanker, R., & Kumari, A. (2023). Microbes-mediated sulphur cycling in soil: Impact on soil fertility, crop production and environmental sustainability. Microbiological Research, 271, 127340.
[32] Aoyu Liu & Yaying Zhang. (2024). An efficient spatial-temporal transformer with temporal aggregation and spatial memory for traffic forecasting. Expert Systems With Applications,250,123884-.
[33] Xiangyuan He,Chen Zhou,Mingzhu Gao,Saisai Sun,Chiying Lyu & Xiaoyi Han. (2025). A method for preserving three spatial features in the upscaling of categorical raster data. Computers and Geosciences,201,105933-105933.